Science and Technology, 1 (1996) 47-53

Magnetism in Iron-Zirconium Systems

M. E. Elzain, A. D. Al Rawas, A. A. Yousif, and A. Gismelseed

Department of Physics, College of Science, Sultan Qaboos University, P.O.Box 36, Al-Khod 123, Muscat, Sultanate of Oman.

خلاصة : استخدمت طريقة المتغيرات المنفصلة لحل معادلة كوهن - شام ذات التقريب المغزلي المحلي للكثافة وذلك لثلل حديد - زركونيوم وحديد - زركونيوم - هايدروجين ، والتي تمثل خليط الحديد والزركونيوم ، والخليط المهدرج . ولقد وجد أن العزم المغناطيس الموضعي والمجال مفرط الدقة عند موضع الحديد تتناقص ، كما وأن كثافة الشحنة التلامسية وعدد الالكترونيات تزداد باضافة الزركونيوم . يكتسب الزركونيوم في الثلل كثيفة الحديد عزما مغناطيسيا سالبا عند حبس الهايدروجين في الفجوات التي تلي جوار الحديد ويزداد العزم المغناطيسي وكذلك المجال مفرط الدقة وتتناقص كثافة الشحنة التلامسية . ونجد العكس عند حبس الهايدروجين في الفجوات المجاورة مباشرة للحديد . أما بالنسبة للزركونيوم فإن قيمة العزم المغناطيسي تقل عند حجز الهايدروجين بجواره مباشرة . نستخلص من هذه الحسابات والمقارنه بالتجارب ان الهايدروجين ، يحبس عند الفجوات التي تجاور الزركونيوم مباشرة وتكون في نفس الوقت في الجوار التالي للحديد .

ABSTRACT: The discrete variational method is used to solve the Khon-Sham equation in the spin-polarized local density approximation for Fe-Zr and Fe-Zr-H clusters, representing iron-zirconium and hydrogenated iron-zirconium alloys. The local magnetic moment and hyperfine field at the Fe site were found to decrease, whereas the contact charge density and occupation number were found to increase with Zr contents. The Zr site in clusters with high Fe contents acquires a negative magnetic moment. When H is trapped at an interstitial site next-neighbouring an Fe atom, the magnetic moment and hyperfine field are enhanced, while the contact charge density is reduced. The opposite occurs when H occupies a neighbouring interstitial site to Fe. For Zr atoms the local magnetic moment is found to become less negative with H at the neighbouring position. We conclude from this calculation that H is trapped in Fe-Zr systems at positions which are nearest to Zr and next-nearest to Fe atoms.

Hydrogen storage in metals is an area of the utmost importance. Since hydrogen is a versatile fuel, its efficient storage and utilization, as a future alternative clean energy source, is a major challenge (Wiswall, 1978). Introduction of hydrogen in metals changes their physical properties. Hydrogen usually enters at the interstitial sites in metals and may eventually lead to the formation of metallic hydrides. To study the effect of hydrogen on the physical properties of metallic alloys the determination of the preferable locations of hydrogen relative to the different components of the alloy as well as its charge state are needed.

Iron-zirconium alloys are known to absorb significant quantities of hydrogen. The base material with zirconium atomic concentration of about 10% is itself a complicated system. It is an amorphous material with a complex magnetic structure. The alloy, which is paramagnetic at high temperatures, turns ferromagnetic at about 250 K and exhibits a spin-glass behaviour at low temperatures (Kaul *et al.*, 1992). The physical mechanism underlying the spin-glass transition is not well understood. Three models are proposed to understand the formation of the spin-glass phase. In one model the ferromagnetic order in the longitudinal direction coexists with a disordered phase in the transverse direction. The two other models are based on magnetic clusters embedded in a ferromagnetic matrix. The clusters in one model are due to concentration fluctuation, and each cluster has internal antiferromagnetic order; whereas clusters in the other model result from density fluctuation, and each cluster possesses an internal ferromagnetic order. In the latter model the clusters are randomly oriented relative to the ferromagnetic matrix. Based on Mossbauer spectroscopy measurements, Kaul *et al.* (1992) have argued in favour of the latter model as the most suitable one for the description of the spin-glass phase.

Beyond a critical atomic concentration of zirconium (~ 60%), the addition of further zirconium converts iron from ferromagnetic to paramagnetic even at low temperatures. On hydrogenation, iron-zirconium alloys with concentration in the paramagnetic range become ferromagnetic (Ostrasz *et al.*, 1994). The question here is what makes the addition of a nonmagnetic component to a nonmagnetic matrix induce ferromagnetic order. This question has been answered for the corresponding iron-vanadium alloy (Elzain *et al.*, 1989). It was found there that hydrogen resides at the octahedral sites neighbouring vanadium and at the same time next-neighbouring iron. Hydrogen then reduces the induced antiferromagnetic moment of vanadium and concomitantly increases the

iron moment, resulting in a net magnetic moment of iron-vanadium system.

Krey *et al.* (1990) have calculated the local magnetic moments at both Fe and Zr sites in clusters representing amorphous iron-zirconium alloys using a tight-binding Koster-Slater parametrized procedure. The magnetic moment is split into longitudinal and transverse components along the lines of the first model describing Fe-Zr alloys. The longitudinal component of the spin moment is parallel to the direction of magnetisation, while the transverse component is perpendicular. The distribution of the longitudinal component of the magnetic moment exhibits two peaks. One peak is centred around the Zr moment of -0.35, in agreement with the results of Drittler *et al.* (1989) for Zr in BCC iron. The other peak shifts with Zr concentration and hydrogenation. The small transverse component of the magnetic moment was found to vanish on hydrogenation. Furthermore, the average magnetic moment per Fe atom was found to decrease linearly with Zr concentration.

In this paper we use the first principle discrete variational method to calculate the local magnetic moments and hyperfine fields at iron and zirconium sites in BCC iron-zirconium alloys. In addition, the average magnetic moment per atom and the hyperfine field at iron site as well as their distributions are calculated. The theoretical model employed in the calculation is presented in section 2, while the results are presented and discussed in section 3. A concluding remark is given in the last section.

Theoretical Model

It is difficult to calculate from first principles the electronic and magnetic properties of a truly amorphous system. In this paper we have studied these properties in terms of distorted BCC, FCC and HCP lattices. The calculations have been performed using both low-and high-symmetry groups. The low-symmetry groups offer flexibility in varying the number of nearest neighbours by selecting suitable interatomic distances. However, we have found that the type of crystal structure utilized is more important to these properties than the variations in the interatomic distances within one crystal type.

The alloys are represented by clusters of atoms consisting of a central atom plus the atoms at the two neighbouring shells. An Fe-centred cluster in a distorted BCC lattice is denoted by FeBCC [N,M], where N and M are the numbers of Fe atoms at the nearest and next-nearest neighbour shells, respectively. A similar notation is adopted for Zr-centred clusters and Fe- and Zr-centred clusters with other crystal structures.

Hydrogen is added interstitially at nearest and next-nearest octahedral positions in the distorted BCC and FCC lattices. Figure 1 depicts the octahedral locations O1 and O2 in the regular BCC lattice. The effect of hydrogen on the HCP structures is not considered.

The discrete variational method (Ellis et al., 1970, and references therein), in the local density approximation, is used to calculate the eigenstates of Kohn - Sham equation with the von Barth - Hedin exchange - correlation potential representing iron-zirconium and iron-zirconium - hydrogen systems. The self-consistent calculation was performed using as variational basis a linear combination of atomic orbitals 3d, 4s, and 4p at Fe sites and 4d, 5s and 5p at Zr sites; while the core states were kept frozen. The matrix elements of the Hamiltonian and overlap matrices were obtained by numerical integration. The pseudo -random diophantine integration method is augmented as desired by a special integration scheme in a spherical volume about particular atoms. Average properties such as the atomic configuration, energy levels, and magnetic moments converge rapidly with the diophantine sample, with 300 to 400 points per atom being sufficient to determine such properties to better than experimental precision. Properties such as contact spin and charge densities which depend sensitively upon the wave function in the atomic core region require a more careful solution of the Kohn-Sham equation in the region of the probe nucleus. In this region the diophantine points are replaced by a dense regular (angular x Gaussian quadrature) mesh.

The contributions to the magnetic hyperfine field B_{hf} at the iron site result mainly from the Fermi contact term.

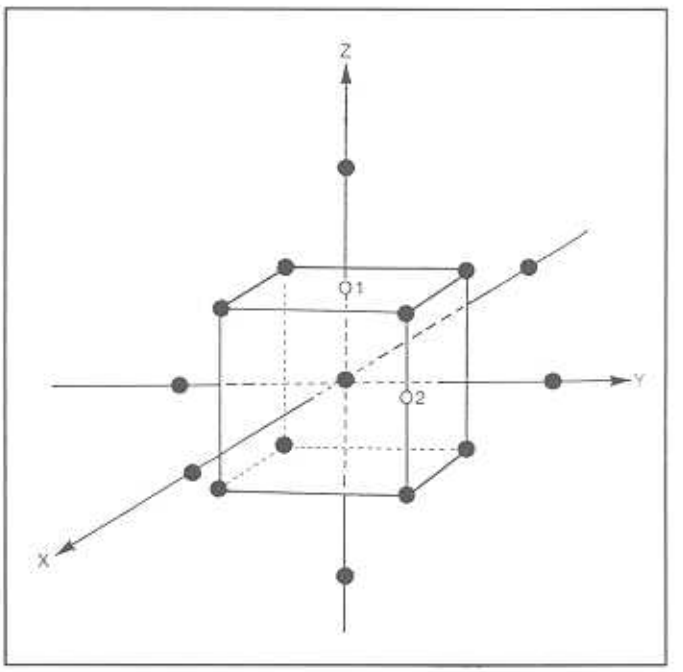

Figure 1. The 15 atom BCC structure showing a central atom and two neighboring shells of atoms (full disks) with H at nearset and next - nearest octahedral interstital positions O1 and O2 (empty disks).

TABLE 1(a)

The3d and 4sp occupation numbers n_d and n_{sp} ; the 3d and 4sp magnetic moments μ_d and μ_{sp} in μ_B ; the contact valence charge density ρ in au; and the magnetic hyperfine field B_{hf} in Teslas, at iron central site in BCC Fe-Zr clusters.

	FeBCC[8,6]	FeBCC[8,0]	FeBCC[0,6]	FeBCC[0,0]
n_d	6.85	6.77	7.19	7.22
n_{sp}	0.49	0.67	1.00	1.49
μ_d	2.60	2.78	1.30	0.07
μ_{sp}	- 0.20	- 0.05	0.06	- 0.02
ρ	4.94	5.93	7.96	7.75
B_{hf}	-39	- 2	+ 20	-2

TABLE 1(b)

The 4d and 5sp occupation numbers n_d and n_{sp}, and the 3d and 4sp magnetic moments μ_d and μ_{sp} in μ_B, at the Zr central site in Zr-Fe clusters.

	ZrBCC[8,6]	ZrBCC[8,0]	ZrBCC[0,6]	ZrBCC[0,0]
n_d	3.23	3.32	4.15	4.36
n_{sp}	0.29	0.33	0.90	1.01
μ_d	0.58	- 0.42	-0.02	0.00
μ_{sp}	- 0.28	- 0.15	-0.02	0.00

This is the difference between spin-up and spin-down densities at the origin. Each spin density, Δρ, can be split into core and valence component. The core contribution scales linearly with the local 3d moment (Blügel *et al.*, 1987; Elzain *et al.*, 1986). Since in our calculation the core states are frozen we estimate the core contribution to B_{hf} from the local 3d moment; while the valence contribution is directly computed. The core contribution is obtained from $B_c = -A\mu_d$, $(A \sim 10\ T\mu_B^{-1})$; whereas the valence part is given by $B_v = B\,\Delta\rho$, $(B = 52.4)$ (Elzain *et al.*, 1986).

Results and Discussion

In the following subsection we present results for the base iron-zirconium clusters; whereas results for hydrogenated clusters are presented in the subsequent subsection.

Fe-Zr CLUSTERS: Table 1 (a) shows the calculated 3d and 4sp occupation numbers and the local magnetic moments obtained using a Mulliken population analysis in hydrogen-free Fe-Zr BCC clusters at the central Fe site. The contact valence charge density and magnetic hyperfine field are also shown. Since the interatomic distances in zirconium are larger than the corresponding iron distances we have used an expanded lattice. The results shown in this and the following tables are for a regular BCC structure with a lattice constant of 5.7 au. We note that the total magnetic moment of the FeBCC [8,6] cluster is larger than the α-iron moment by about 10% due to this lattice expansion. By fixing the lattice constant for all clusters we can ascribe any changes in the physical quantities to the chemical effects of the added atoms.

We observe that the total occupation numbers at the Fe site increase with Zr atoms in agreement with the Pauli electronegativity scale. However, the 3d local moment at the Fe site decreases due to a reduction in exchange splitting resulting from the mixing of Fe and Zr 3d-4d orbitals. The 4d level of Zr lies above Fe 3d level (Clementi *et al.*, 1974), and it mixes strongly with the Fe minority level. This leads to a negative polarization of the Zr atom and to a shift down of the Fe minority level. Consequently, electrons from the Fe majority level are transferred to the minority level resulting in the reduction of the Fe local moment. This is exhibited in Table 1(a). The partial 3d density of states at the Fe site depicted in figure 2(a) also reflects the same trends. The minority energy levels are pushed towards the majority levels, and when the surrounding atoms are Zr the levels overlap.

The contact charge density at the central Fe site increases with increasing Zr, leading to a negative isomer shift, in agreement with experimental results (Fujinami *et al.*, 1986). Volume expansion should result in a reduction of contact density relative to the unexpanded lattice. Hence this increase is mainly a chemical effect and results from the increase in the s-like valence electrons. The magnitude of the contact hyperfine field decreases with increasing Zr contents, and for FeBCC[0,6] clusters its orientation is parallel to the local magnetic moment.

We also notice that the local 3d moment at FeBCC[8,0] is larger than that of FeBCC[8,6]; whereas the contact hyperfine field is very small. This large variation in B_{hf} is attributed to the strong dependence of the s-like valence contribution on the local environment (Elzain *et al.*, 1986). The presence of Zr at the nearest and next-nearest neighbours of Fe reduces B_{hf} by about 6 to 8 T per added atom. However, the Fe local moment barely changes by the appearance of Zr at the next-nearest position and decreases when the neighbouring position is occupied.

The Zr-site properties exhibit the behaviour expected on the grounds of electronegativity and 3d-4d orbital mixing. In table 1(b) we show the occupation numbers and the local moments induced at the Zr site. The local 4d moment is negative and larger than that calculated by Drittler *et al.* (1989), because we have used an expanded

lattice. A comparable value to that in Drittler *et al.* (1989), is obtained when the α-iron lattice constant is used. The occupation number at the central Zr site in BCC zirconium is larger than the corresponding free-atom occupation, which means that the central atom gains some charge from its neighbours. However, in an HCP structure with the zirconium lattice constant, we found that the occupation numbers are $n_d = 3.21$ and $n_{sp} = 0.75$, which gives an almost neutral Zr-site in zirconium. At the Zr-site charge is transferred from the sp orbital to the d orbitals. The local magnetic moment at Zr in zirconium for both BCC and HCP configurations is zero. The partial d density of states at the Zr-site in a BCC structure is shown in figure 2(a). The density clearly indicates a negative polarization at Zr in iron (lower curves) and a zero moment in zirconium (upper curves). Moreover, the local properties at the Fe and Zr sites in FCC structures were calculated and similar trends were found, except for the occurrence of Fe-Fe antiferromagnetic coupling in some configurations.

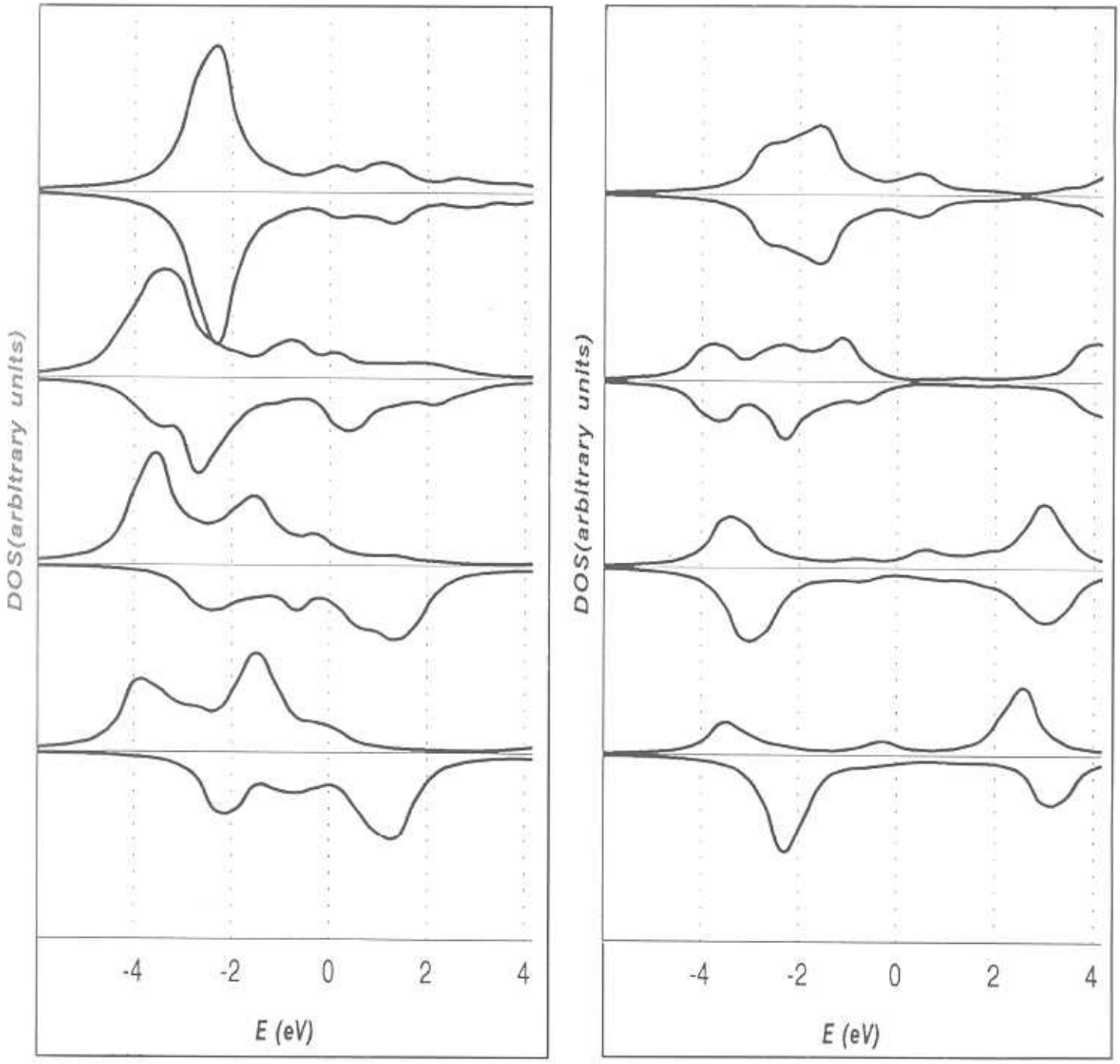

Figure 2(a). The partial 3d density of states at Fe site for Fe-Zr clusters: In each set of two curves the upper one represents the majority states and the lower one the minority states. The bottom set represent FeBCC86 cluster followed in upward direction by FeBCC80, FeBCC06 and FeBCC00 respectively. **Figure 2(b).** The 3d partial density of states at Zr site in Zr-Fe clusters: The bottom set of curves represents ZrBCC86 cluster followed in upward direction by ZrBCC80, ZrBCC06 and Zr-BCC00 respectively.

The average and probability distributions of magnetic moments and hyperfine fields in Fe-Zr are calculated by taking a binomial distribution. The average magnetic moment, which is shown in figure 3, is found to decrease linearly with Zr concentration at a rate of about $3.3\mu_B$ per unit atomic concentration, in agreement with Krey *et al.* (1990). The probability distribution of local magnetic moments is depicted in figure 4 for Zr concentration of c=0.1. It exhibits two peaks centred at average Zr and Fe moments. On the other hand, the distribution of magnetic hyperfine field, which is related to the Fe site only, also shows two peaks (figure 5 for c=0.1.). These latter peaks cannot be obtained by scaling the Fe moment by a factor of about 14.5 T per Bohr magneton as suggested in Krey *et al.* (1990). A single peak would have resulted in this case. This argues against a linear correspondence between Fe local moments and the hyperfine field shown by the local values in Table 1(a). From the comparison of measurements of magnetization and the magnetic hyperfine field, Kaul *et al.* (1992) have also argued against a linear scaling between μ and B_{hf}. The two peaks in B_{hf} distribution are centred around 35 T and 28 T which are attributed to Zr-free Fe sites and Fe sites with one Zr atom on each neighbouring shell on the average. Unlike the peaks identified in Kaul *et al.* (1992) as one being due to a Zr-rich iron matrix whereas the other is due to an embedded iron-rich ferromagnetic cluster, the two peaks here occur in a homogeneous alloy. However, the spin-glass transition cannot be explained in such a system with low Zr concentration unless a structural change to FCC is allowed for. Henceforth, the second model becomes viable and the spin-glass transition results from an internal antiferromagnetic order.

Fe-Zr-H CLUSTERS: The effect of hydrogen on the electronic and magnetic properties of Fe-Zr clusters in BCC and FCC structures has been considered. Hydrogen is assumed to occupy an octahedral site neigbouring (O1) or next-neighbouring (O2) a central atom. In table 2(a) we present results for a regular BCC Fe-centered clusters with a lattice constant $a = 5.7$ au and H at the O2 site. We note that the occupation numbers at Fe site barely change compared to the corresponding H-free clusters [Table 1(a)]. On the other hand, H at the O2 site generally increases the Fe magnetic moment. In particular, Fe-centred clusters with Zr at the first shell experience a large increase in the magnetic moment, while the changes

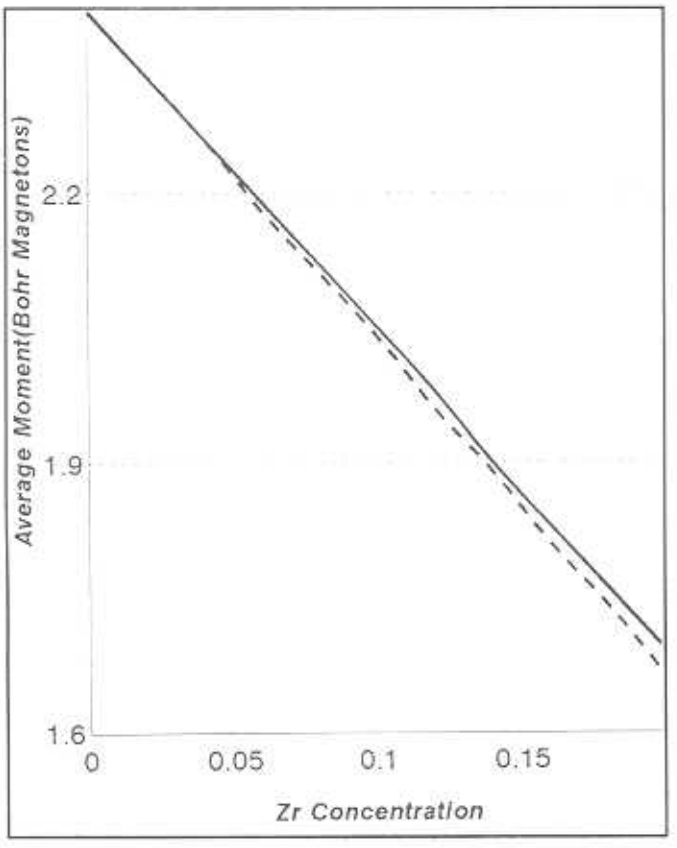

Figure 3. The average magnetic moment in Fe-Zr system calculated using a random distributiion of Zr atoms in the BCC lattice. The dashed curve represents the hydrogen free system whereas the solid curve represents hydrogenated systems.

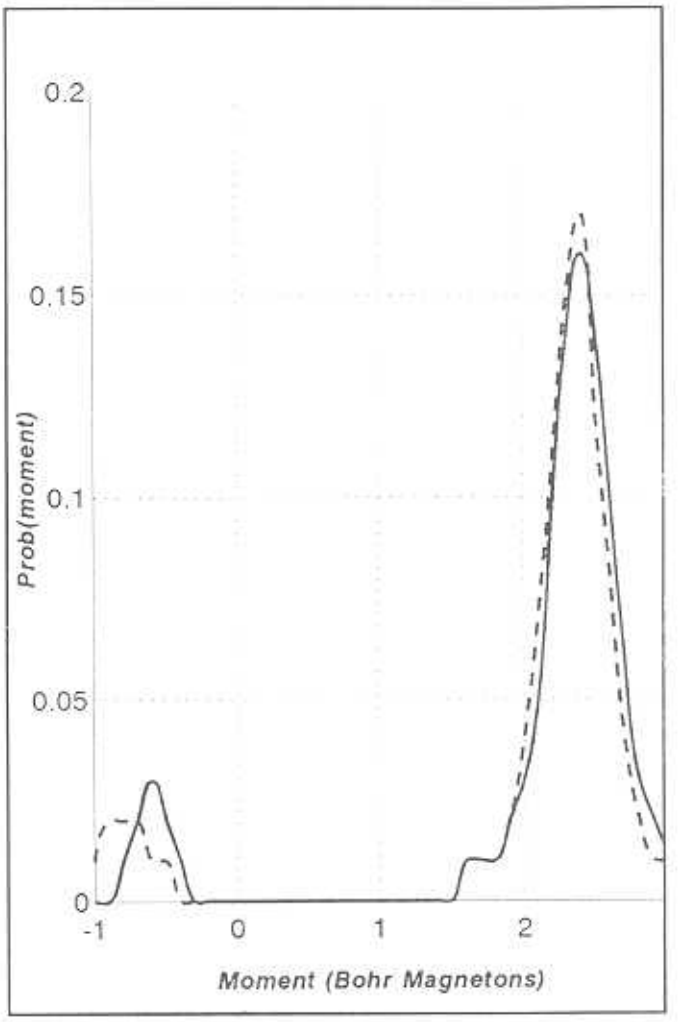

Figure 4. The local magnetic moment distribution is obtained using a random distribution of Zr in the BCC lattice. The dashed curve represents the H free case and the continuous curve represents hydrogenated systems.

TABLE 2(a)

The 3d and 4sp occupation numbers n_d and n_{sp}; the 3d and 4sp magnetic moments μ_d and μ_{sp} in μ_B; the contact valence charge density ρ in au; and the magnetic hyperfine field B_{hf} in Teslas, at iron central site in BCC Fe-Zr-H clusters with H at the octahedral position O2.

	FeBCC[8,6]	FeBCC[8,0]	FeBCC[0,6]	FeBCC[0,0]
n_d	6.85	6.84	7.21	7.34
n_{sp}	0.43	0.56	1.00	1.41
μ_d	2.79	2.55	1.31	0.60
μ_{sp}	- 0.16	- 0.02	0.09	- 0.01
ρ	4.84	5.42	7.78	7.51
B_{hf}	-32	- 11	+ 18	-3

for clusters with Fe at the first shell are minor. We found that one 3d orbital at the Fe site mixes with the 1s H orbital. This mixing lowers the corresponding majority spin state near the Fermi level, resulting in a full level on hydrogenation compared to an empty one for the

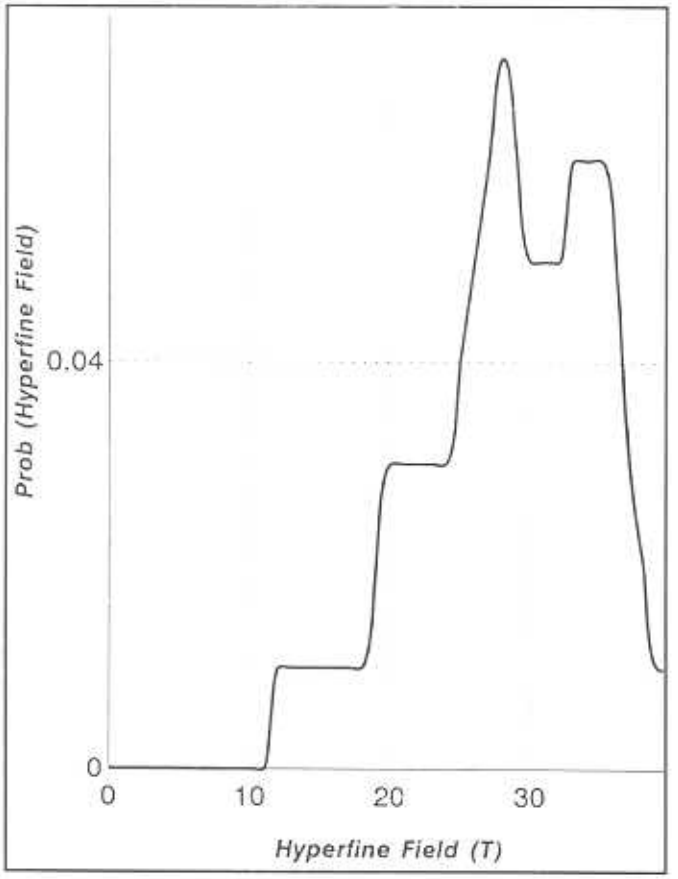

Figure 5. The distribution of the magnetic hyperfine field at Fe sites in Fe-Zr systems calculated using a random binomial distribution of Zr in the BCC lattice. Both H free and hydrogenated systems have similar curves.

TABLE 2(b)

The 4d and 5sp occupation numbers n_d and n_{sp}; and the 3d and 4sp magnetic moments μ_d and μ_{sp} in μ_B, at the Zr central site in Zr-Fe-H clusters with H at the O1 position.

	ZrBCC[8,6]	ZrBCC[8,0]	ZrBCC[0,6]	ZrBCC[0,0]
n_d	3.67	3.66	4.44	4.71
n_{sp}	0.01	0.00	0.55	0.65
μ_d	- 0.43	- 0.31	- 0.01	0.11
μ_{sp}	0.00	0.00	0.00	0.00

equivalent H-free cluster. Moreover, we have calculated the local properties of Fe-centred cluster with H at O1 sites. The occupation numbers are found to increase slightly in the latter case as compared to H at O2 sites and H-free clusters. The local moment decreases for clusters with Fe in the neighbouring shell and increases, but remains less than the corresponding O2 case, when Zr is at the first shell. An expanded and also a slightly compressed BCC lattice retains similar features, indicating that the most prominent changes result from the presence of H itself rather than from the associated volume distortion. In addition, we found that H at the neighbouring octahedral site in the FCC structure removes some of the Fe-Fe antiferromagnetic couplings present in the unhydrogenated clusters. This will consequently lead to an increase in the average magnetic moment.

The contact charge density at the Fe site slightly decreases when H resides at the O2 site, leading to a less negative isomer shift, in agreement with Aubertin *et al.* (1988), where the isomer shift for hydrogenated Zr_3Fe has been found to vary from about -0.3 mm s^{-1} to about +0.2 mm s^{-1} with increasing hydrogen contents. We note here that this behaviour contradicts the predictions of volume effects which should lead to a higher density due to the presence of the additional H atom. The variations in the contact hyperfine field are minor, and the distribution of B_{hf} exactly overlaps the H-free case shown in figure 5.

The effect of H on the Zr site is more pronounced. We show in table 2(b) the local properties at the Zr site with H at the O1 position. The 3d occupation numbers are enhanced, while the sp occupations are reduced in relation to the unhydrogenated clusters [Table 1(b)]. The local magnetic moments become less negative. These changes are brought by the transfer of the sp electrons at the Zr site to 3d orbitals. Since the 5s and 4d levels of the Zr atom in the $5s^14d^3$ configuration are almost degenerate (Clementi *et al.*, 1974), the 5s electrons mix more strongly with the low-lying H orbitals and are pushed up in energy. This interaction removes the sp-d degeneracy and leads to charge transfer to the 4d Zr level. The

transferred electrons occupy minority states and consequently lead to a reduction in the magnetic moment. The reduction in the magnitude of the induced Zr moment, combined with the enhancement of Fe moment result in an increased net moment of the Fe-Zr alloys on hydrogenation. The average magnetic moment in hydrogenated alloys increases slightly with Zr concentration, as shown in figure 3 for H concentration of about 6%. The distribution of the magnetic moments also reflects the reduction of the Zr moment and the slight increase of the Fe moment, as shown in figure 4. We conclude from these findings that hydrogen in Fe-Zr alloys is trapped at interstitial positions which are neighbouring Zr atoms and at the same time next-neighbouring Fe atoms.

Conclusion

The local properties at iron and zirconium sites in Fe-Zr and Fe-Zr-H clusters in distorted and regular structures have been calculated. The occupation numbers and contact charge density at the Fe site are found to increase with increasing Zr contents leading to negative isomer shifts. The local Fe magnetic moment and the magnetic hyperfine field are reduced, and for some configurations in the FCC structure, the Fe-Fe coupling turns antiferromagnetic. The relation between the local moment and the hyperfine field is found to be nonlinear and, hence, the hyperfine field cannot be determined from the knowledge of the local moment. This is clearly illustrated by cases in which the moment is enhanced, whereas the magnitude of the hyperfine is reduced. A negative moment is induced at the Zr site when neighbouring atoms are Fe. This moment decreases in magnitude and vanishes with an increasing number of Zr atoms in the surroundings. When hydrogen is included in the Fe-Zr clusters its influence depends on the position it occupies. At the Fe sites, the trapping of H at the neighbouring interstitial position reduces the local moment and the hyperfine field and at the same time enhances the occupation numbers and contact charge densities. If H is trapped at the next-neighbouring interstitial position of Fe then the opposite effects occur. For the Zr site the induced magnetic moment becomes less negative when H is at the nearest position. It is concluded from such trends and from a comparison to experimental results that H is trapped at interstitial sites which are neighbouring Zr atoms and next-neighbouring Fe atoms.

References

AUBERTIN F., A. ABEL., S. J. CAMPBELL, and U. GONSER, 1988. *Hyperfine Interactions* **41**, 543.

BLÜGEL S., H. AKAI, R. ZELLER, and P.H. DEDERICHES, 1987. *Phys. Rev* B **35**, 3271.

CLEMENTI E and C. ROETTI, 1974. *Atomic Data and Nucl. Data Tab* **14**, 177.

DRITTLER B., N. STEFANU, BLÜGEL S., R. ZELLER, and P. H. DEDERICHS, 1989. *Phys. Rev.* B **40**, 8203.

ELLIS D. E. and G.S. PAINTER, 1970. *Phys. Rev.* B **2**, 2887.

ELZAIN M.E. and B. LINDGREN, 1989. *J. Phys. (Condensed Matter)* 1, 7055.

ELZAIN M.E. and D.E. ELLIS, and D. GUENZBERGER, 1986. *Phys. Rev* **34**, 1430.

FUJINAMI M. and Y. UJIHIRA, 1986. *J. Appl. Phys.* **59**, 2387.

KAUL S. N., V. SIRUGURI, and G. CHANDRA, 1992. *Phys. Rev* B **45**, 12343.

KREY U, S. KROMPIEWSKI, and U. KRAUSS, 1990. *J. Mag. Mag. Mater.* **86**, 85.

OSTRASZ A. and M. SZUSZKIEWICS, 1994. *Hyperfine Interactions* **94**, 2287 (1994).

WISWALL R., 1978, in *Hydrogen in Metals II* (edited by G Alefeld and J. Volkl), Topics in Applied Science, *Vol.* **29** p. 201. Springer - Verlag, Berlin (1978).

Received 1 January 1996
Accepted 9 July 1996